LANGMUIR
Article
Cite This: *Langmuir* 2019, 35, 3840−3847
pubs.acs.org/Langmuir

Connect the Thermodynamics of Bulk and Confined Fluids: Confinement-Adsorption Scaling

C. Z. Qiao,[†,‡] S. L. Zhao,[*,†] H. L. Liu,[§] and W. Dong[*,‡]

[†]State Key Laboratory of Chemical Engineering and School of Chemical Engineering, and [§]School of Chemistry and Molecular Engineering, East China University of Science and Technology, 130 Meilong Road, 200237 Shanghai, China

[‡]Université de Lyon, CNRS, Ecole Normale Supérieure de Lyon, Université Lyon 1, Laboratoire de Chimie, UMR 5182, 46, Allée d'Italie, 69364 Lyon Cedex 07, France

ABSTRACT: A fluid (a gas or a liquid) adsorbed in a porous material can behave very differently from its bulk counterpart. The advent of various synthesized materials with nanopores and their wide applications have provided strong impetus for studying fluids in confinement because our current understanding is still incomplete. From a large number of Monte Carlo simulations, we found a scaling relation that allows for connecting some thermodynamic properties (chemical potential, free energy per particle, and grand potential per particle) of a confined fluid to the bulk ones. Upon rescaling the adsorbed fluid density, the adsorption isotherms for many different confining environments collapse to the corresponding bulk curve. We also reveal the intimate connection of the reported scaling relation to Gibbs theory of inhomogeneous fluids and morphological thermodynamics. The advance in our understanding of confined fluids, gained from this study, also opens attractive perspectives for circumventing experimental difficulty for directly measuring some fluid thermodynamic properties in nanoporous materials.

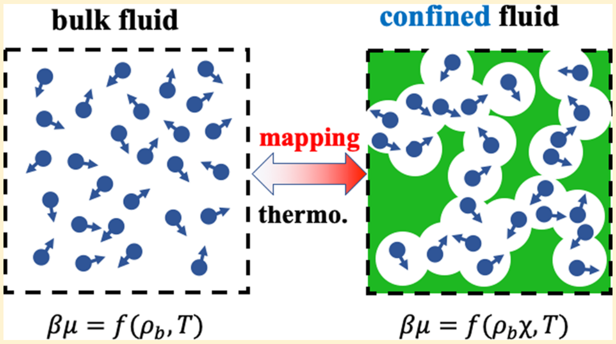

1. INTRODUCTION

Porous materials have many important applications.[1−4] For example, absorbing hydrogen in a porous material has been proposed as a possible strategy for developing a H_2-based clean new energy source.[3] Since long time, various zeolites have been used as molecular sieves and catalysts. Because of the specific pore size and topology, high selectivity is imparted to the zeolite-based catalysts. Such selectivity is extensively exploited in various chemical processes, for example, catalytic cracking in oil industry.[4] Nowadays, it is widely recognized that the properties of fluids confined in porous media can be dramatically different from those of the bulk ones.[5−26] Understanding the behavior of confined fluids is important not only from a fundamental point of view but also for conceiving innovative industrial processes.

Accompanying the elaboration of high-performance functionalized nanoporous materials, a large number of experimental and theoretical investigations have been carried out during the last decades. Nevertheless, our understanding of confined fluids is still incomplete. Currently, we do not really know to which extent thermodynamics can be still applied at the scale of nanopores. Different aspects of confined fluids are being studied in a case-by-case way. It can be readily admitted that the fluid−solid interface and the fluid inhomogeneity near it have to be taken into account. For fluid adsorption in real porous materials, the fluid−solid interfaces are generally curved ones. It might appear surprising that the thermodynamics for dealing with curved interfaces is not so well established, although early investigations go back to Tolman.[27] Mecke and co-workers have made efforts to develop a general framework, named morphological thermodynamics, to account for a more complex surface morphology.[28−32] The foundation of morphological thermodynamics has been questioned recently.[33−36] To our best knowledge, no experimental measurement has ever been made to determine the bending rigidity coefficients needed in morphological thermodynamics method for any fluid−solid interface.

A large literature exists on the study of confined fluids by theoretical and simulation methods[5−26,37−64] (references given here are just for illustration but far from being exhaustive). Models with simple pore geometry (e.g., slit or cylinder) are widely studied. In such models, pore size distribution and connectivity among pores are neglected. Fluid adsorption and diffusion in an ordered porous material, for example, zeolites, have been studied by simulations. To account for the quenched disorder, models for random porous media have been proposed also, for example, Madden−Glandt model and various variants.[37−42] Despite these considerable efforts, it is unfortunate to note that no unifying picture of various confined fluids has emerged. Today, we do not yet have a

Received: September 13, 2018
Revised: January 28, 2019
Published: January 29, 2019

DOI: 10.1021/acs.langmuir.8b03126
Langmuir 2019, 35, 3840−3847

precise idea about the respective roles played by pore connectivity, pore size distribution, pore morphology, or quenched disorder. In a bulk fluid, a molecule is surrounded by other fluid molecules while in a fluid adsorbed in a porous solid, a large number of fluid molecules are located near a fluid−solid interface. These molecules feel the interaction with both fluid and solid molecules. The nature of the fluid−solid interaction can vary significantly, from repulsive to attractive ones. This additional interaction can make the confined fluid behave very differently from the corresponding bulk one. Although a confined fluid appears complicated because of the complex confining environment of the adsorbent, one can wonder if there is any connection between confined and bulk fluids. Currently, we know quite few about this. Acquiring such knowledge does not only advance our understanding about these complex systems but also can have important applications. In this article, we report several relations that allow for connecting some properties of a confined fluid to those of a bulk one. By rescaling the density of a confined fluid, the adsorption isotherms (also free energy or grand potential per particle) of fluids in a large variety of confining environments can collapse to the corresponding bulk ones.

2. MODEL AND METHOD

We investigated the thermodynamic properties (chemical potential, Helmholtz free energy, and grand potential) of confined fluids by considering a large variety of models [hard sphere (HS) or Lennard-Jones (LJ) fluids in slit pores, ordered or disordered porous matrices]. Simulations were carried out with the help of Monte Carlo methods (in grand canonical or canonical ensembles). The details about the models and computational conditions are given in Appendix.

3. RESULTS AND DISCUSSION

Inspired by the exact and analytical results for some models (ideal gas in a variety of confining environments) and scrutinizing our simulation results for many more complex-confined fluids with interatomic interactions, we found the following scaling relation:

$$\beta\mu(\chi\rho,\, T) = \beta\mu^{\text{bulk}}(\rho,\, T) \tag{1}$$

$$\beta f(\chi\rho,\, T) = \beta f^{\text{bulk}}(\rho,\, T) \tag{2}$$

$$-\beta\omega(\chi\rho,\, T) = Z^{\text{bulk}}(\rho,\, T) \tag{3}$$

where $\beta = 1/(k_\text{B}T)$ (k_B: Boltzmann constant, T temperature), μ and μ^{bulk} are the chemical potentials of confined and bulk fluids, respectively, ρ is the number density of the bulk fluid in equilibrium with the confined one ($\rho = N/V$, V: volume), f and f^{bulk} are free energy per particle of confined and bulk fluids, respectively, that is, $f = F/N^{\text{conf}}$, and $f^{\text{bulk}} = F^{\text{bulk}}/N$ (N^{conf}: particle number of confined fluid), ω is the grand potential per particle of a confined fluid, Z^{bulk} is the compressibility factor in the bulk, that is, $Z^{\text{bulk}} = \beta P^{\text{bulk}}/\rho$, ($P^{\text{bulk}}$: bulk fluid pressure, note that the compressibility factor is simply the negative of grand potential per particle). The scaling factor is given by

$$\chi = \phi_0 + \Gamma A/(\beta P^{\text{bulk}} V) \tag{4}$$

where ϕ_0 is the geometric porosity of the porous adsorbent under consideration (see ref 49 for definition), Γ is the excess adsorption amount per unit surface area, and A is the area of the fluid−solid interface of the confined fluid. ΓA can be calculated simply from

$$\Gamma A = (\rho^{\text{conf}} - \phi_0\rho)V \tag{5}$$

where $\rho^{\text{conf}} = N^{\text{conf}}/V$. It is to note that only ΓA is needed but not Γ and A separately and ΓA can be measured experimentally. When the second term on the right-hand side (rhs) of eq 4 is dropped out, we have immediately

$$\beta\mu(\phi_0\rho,\, T) = \beta\mu^{\text{bulk}}(\rho,\, T) \tag{6}$$

$$\beta f(\phi_0\rho,\, T) = \beta f^{\text{bulk}}(\rho,\, T) \tag{7}$$

$$-\beta\omega(\phi_0\rho,\, T) = Z^{\text{bulk}}(\rho,\, T) \tag{8}$$

We name this as pure confinement scaling, which holds rigorously for an ideal gas in hard matrices, for example, a HS, an overlapping HS (OHS), or a hard sponge matrix. From a scaled particle theory,[46−51] we can show that the pure confinement scaling also holds for HS fluids confined in HS and OHS matrices when the size ratio of matrix to fluid particle is large.[51] Although one can readily see the physical meaning of the first term in the scaling factor, the significance of the second term appears less trivial. In fact, it is a measure for the ratio of the volume of the inhomogeneous region near the fluid−solid interface with respect to the total volume of the porous solid sample.

The simulation results presented below demonstrate the validity of the scaling relation given in eqs 1−4, named as confinement-adsorption scaling, for a large variety of confined fluids under broad conditions. To show the general and robust character of this scaling relation, we considered virtually all types of confined fluids, that is, in various porous environments like isolated slit pores, connected ordered or random porous matrices including spongelike ones, and different types of fluid−fluid and fluid−solid interactions (see Appendix for detailed information about the considered systems and simulation conditions).

Figure 1a shows the collapse of adsorption isotherms of a HS fluid confined in 19 different environments to the bulk $\mu \sim \rho$ isotherm after scaling according to eq 1 while Figure 1b presents the results before scaling. The robustness of the

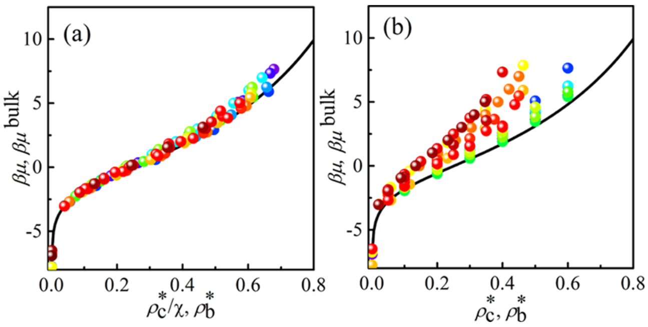

Figure 1. Monte Carlo simulation results for a HS fluid confined in 19 different confining environments (see Appendix for details about considered systems and the corresponding symbols): (a) chemical potential, $\beta\mu$, as a function of scaled density ρ_c^*/χ ($\rho_c^* = \rho^{\text{conf}}\sigma^3$, σ: HS diameter); (b) chemical potential, $\beta\mu$, as a function of nonscaled density ρ_c^*. The full line is the bulk $\beta\mu^{\text{bulk}} \sim \rho_b^*$ isotherm from the Carnahan−Starling equation of state. Subscripts b and c denote the bulk and confined fluids, respectively.

scaling relation is demonstrated by the large diversity of the considered confining environments, from isolated slit pores to random porous matrices with pure repulsive or repulsive plus attractive fluid−solid interactions. To establish the general validity of the scaling relation, we also carried out simulations with a LJ fluid (see results in Figure 2). These results show the general character of the scaling relation, which also holds for fluids with an attractive interaction.

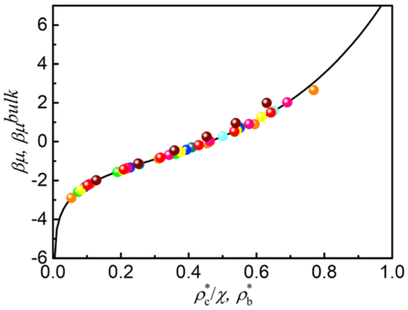

Figure 2. Monte Carlo simulation results for an LJ fluid confined at $T^* = 3.5$ in nine different confining environments (see Appendix for details about considered systems and the corresponding symbols): chemical potential, $\beta\mu$, as a function of scaled density ρ_c^*/χ ($\rho_c^* = \rho^{conf}\sigma^3$, σ: LJ size parameter). The full line is the bulk $\beta\mu^{bulk} \sim \rho_b^*$ isotherm from the equation of state given in ref 65.

The scaling relation holds not only for the adsorption isotherms but also for some other thermodynamic quantities, for example, free energy per particle and grand potential per particle. Figure 3 shows the collapse of βf and $-\beta\omega$ for different confined HS fluids to the corresponding bulk curves. The same scaling relation holding for chemical potential, free energy per particle, and grand potential per particle implies immediately that βf and $-\beta\omega$ collapse to the corresponding bulk curves if they are expressed as a function of chemical potential, that is,

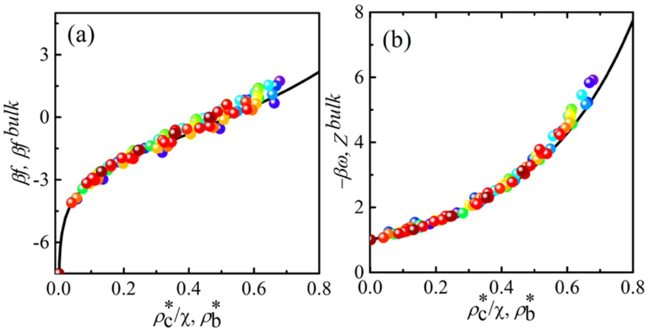

Figure 3. Monte Carlo simulation results for a HS fluid confined in 19 different confining environments (see Appendix for details about considered systems and the corresponding symbols): (a) free energy per particle, βf, as a function of scaled density ρ_c^*/χ ($\rho_c^* = \rho^{conf}\sigma^3$, σ: HS diameter); (b) minus grand potential per particle, $-\beta\omega$, as a function of scaled density ρ_c^*/χ. Full lines are, respectively, the corresponding bulk $\beta f^{bulk} \sim \rho_b^*$ and $Z^{bulk} \sim \rho_b^*$ curves from the Carnahan−Starling equation of state.

$$\beta f(\mu, T) = \beta f^{bulk}(\mu, T) \tag{9}$$

$$-\beta\omega(\mu, T) = Z^{bulk}(\mu, T) \tag{10}$$

This invariance is remarkably illustrated by Figure 4. One obvious importance of such invariance relations is that they allow for determining some thermodynamic functions of a confined fluid from the corresponding bulk ones. It is well-known that the experimental measurement of thermodynamic properties of confined fluids is much more difficult or impossible currently. To our best knowledge, no direct experimental determination of pressure and free energy has ever been made for fluids confined in nanoporous materials.

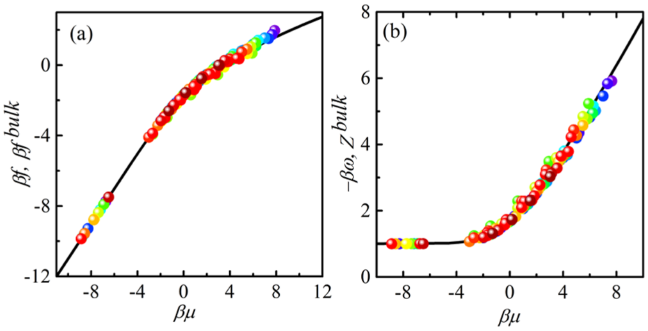

Figure 4. Monte Carlo simulation results for a HS fluid confined in 19 different confining environments (see Appendix for details about considered systems and the corresponding symbols): (a) free energy per particle, βf, as a function of chemical potential, $\beta\mu$; (b) minus grand potential per particle, $-\beta\omega$, as a function of chemical potential, $\beta\mu$. Full lines are, respectively, corresponding bulk $\beta f^{bulk} \sim \beta\mu$ and $Z^{bulk} \sim \beta\mu$ curves from the Carnahan−Starling equation of state.

Although the simulation results presented above establish the validity of the confinement-adsorption scaling and the invariance described by eqs 9 and 10, a derivation of these relations from first principles is currently lacking. Nevertheless, the confinement-adsorption scaling has some intimate connection with Gibbs theory for interfacial systems[66,67] and the morphological thermodynamics advocated by Mecke et al.[28−32] In fact, Gibbs theory can be derived from the scaling relation given in eq 1. We start from the following equivalent form of eq 1:

$$\beta\mu(\rho^{conf}, T) = \beta\mu^{bulk}\left(\frac{\rho^{conf}}{\chi}, T\right) \tag{11}$$

Expanding the rhs of this equation to the first order around ρ^{conf}/ϕ_0, we obtain

$$\begin{aligned}\beta\mu(\rho^{conf}, T) &= \beta\mu^{bulk}\left(\frac{\rho^{conf}}{\phi_0}, T\right) + \left(\frac{\rho^{conf}}{\chi} - \frac{\rho^{conf}}{\phi_0}\right)\frac{\partial[\beta\mu^{bulk}(\rho^{conf}/\phi_0, T)]}{\partial(\rho^{conf}/\phi_0)}\\ &= \beta\mu^{bulk}\left(\frac{\rho^{conf}}{\phi_0}, T\right) + \left(\rho - \frac{\rho^{conf}}{\phi_0}\right)\frac{\partial[\beta\mu^{bulk}(\rho^{conf}/\phi_0, T)]}{\partial(\rho^{conf}/\phi_0)}\\ &= \beta\mu^{bulk}\left(\frac{\rho^{conf}}{\phi_0}, T\right) - \frac{\Gamma A}{\phi_0 V}\frac{\partial[\beta\mu^{bulk}(\rho^{conf}/\phi_0, T)]}{\partial(\rho^{conf}/\phi_0)}\end{aligned} \tag{12}$$

Equation 5 was used when going to the last equality of eq 12. Integrating both sides of the above equation with respect to ρ^{conf} leads to

$$\begin{aligned}\frac{\beta F(N^{\mathrm{conf}}, V, T)}{V} &= \int \beta\mu(\rho^{\mathrm{conf}}, T)\, \mathrm{d}\rho^{\mathrm{conf}}\\ &= \phi_0 \frac{\beta F^{\mathrm{bulk}}(N^{\mathrm{conf}}, V\phi_0, T)}{V\phi_0}\\ &\quad - \int \frac{\Gamma A}{V} \frac{\partial[\beta\mu^{\mathrm{bulk}}(\rho^{\mathrm{conf}}/\phi_0, T)]}{\partial(\rho^{\mathrm{conf}}/\phi_0)}\, \mathrm{d}(\rho^{\mathrm{conf}}/\phi_0)\\ &= \phi_0 \frac{\beta F^{\mathrm{bulk}}(N^{\mathrm{conf}}, V\phi_0, T)}{V\phi_0} + \frac{\beta\gamma A}{V}\end{aligned} \tag{13}$$

where γ is the surface tension at the fluid−solid interface and A the surface area of the pore space boundary used for calculating the porosity, ϕ_0. Gibbs adsorption equation was used when going to the last equality in the above equation. Equation 13 is nothing else but the free energy of the inhomogeneous system expressed as the bulk contribution plus the surface term following Gibbs theory, that is,

$$F(N^{\mathrm{conf}}, V, T) = F^{\mathrm{bulk}}(N^{\mathrm{conf}}, V\phi_0, T) + \gamma A \tag{14}$$

Subtracting μN^{conf} from both sides of the above equation, we also obtain

$$\Omega(\mu, V, T) = \Omega^{\mathrm{bulk}}(\mu, V\phi_0, T) + \gamma A \tag{15}$$

where Ω and Ω^{bulk} denote the grand potential of the confined or bulk fluid, respectively. According to morphological thermodynamics, the grand potential of an inhomogeneous fluid is written as the sum of a bulk term and a surface term with the surface tension including three contributions (a flat surface term plus two curvature terms).[28−32] Although not appearing explicitly in our scaling relation, the surface tension is embodied in it. The above demonstration reveals this unambiguously and thus evidences an intimate connection between our scaling relation and the general theoretical frameworks like Gibbs theory and morphological thermodynamics. At first sight, it may appear surprising that rescaling fluid density alone can account for various fluid−solid interactions. In fact, this interaction is taken into account through the adsorption term, that is, ΓA [see eq 4]. The discussion just given above shows further and explicitly that the interface contribution to the free energy is indeed included in our scaling relation.

Scaling relations have been found previously for some dynamic properties, for example, entropy scaling for the diffusion coefficient of a HS fluid confined in slit pores[68−70] or an LJ fluid in a zeolite,[71] or for the relaxation time of a glass-making liquid in slit pores.[72] Mittal, Errington, and Truskett found that the $D \sim s^{\mathrm{ex}}$ (D: diffusion coefficient; s^{ex}: excess entropy per particle) curves of a HS fluid confined in various slit pores collapse to the bulk curve when the fluid density is calculated with the total volume instead of that accessible to the particle centers.[68] This way to obtain curve collapse is in fact a particular case of the general scaling reported in the present work. First, the situation considered by these authors corresponds to what we called a pure confinement regime, that is, without the second term of the scaling factor given in eq 4. Our investigations show that the general scaling relation holds under wider conditions. Second, applying eq 4 to the particular case of slit pores under the pure confinement regime consists simply in calculating the fluid density by using the total volume as did Mittal, Errington, and Truskett.[68] In a later study, Mittal showed that data collapse to the bulk curve can also be obtained if the diffusion coefficient is plotted as a function of compressibility factor.[72] Our finding reported here provides the thermodynamics foundation for this. It is to note that in the case of a HS fluid, the reduced free energy per particle, βf, is equal to the reduced entropy per particle, s/k_{B}. Therefore, our results are perfectly consistent with those of Mittal et al.[68−70] Moreover, in light of our finding, we can make an immediate prediction that the $D \sim \mu$ curves for confined fluids also collapse to the corresponding bulk one.

4. CONCLUSIONS

Our simulation results establish the validity of a scaling relation for several thermodynamic functions, which connects confined and bulk fluids. The invariance with respect to confining environments is discovered for Helmholtz free energy and grand potential per particle if they are expressed as a function of chemical potential. This confers a particular significance to the use of chemical potential as an independent variable in the study of confined fluids or inhomogeneous fluids. The invariance described by eqs 9 and 10 holds rigorously for an ideal gas confined in various pores under all the allowed thermodynamic conditions. It is really surprising that such invariance also holds when a fluid−fluid interaction is present. Figure 4b shows a pretty good data collapse in the density region where the compressibility factor deviates largely from its value for an ideal gas. It is very intriguing that confined fluids can bear perfectly a hallmark of an ideal gas far beyond the low-density region. Although a derivation of the scaling relation from first principles is currently unavailable, we have revealed its intimate connection with general theoretical frameworks like Gibbs theory or morphological thermodynamics for inhomogeneous fluids. We believe this is why the scaling relation works so well under wide conditions and for a large variety of confining environments. The most significant message conveyed by our results is that the apparently disconnected behaviors of confined fluids are not so disparate but can be nicely organized via scaling. The scaling relation shows clearly that the porosity (space accessibility) and fluid−solid interaction (through the adsorption term) is of primary importance for determining the thermodynamics of confined fluids. The other characteristics, such as pore connectivity, pore shape, pore size distribution, and so forth, play a less significant role. As an immediate and interesting application, our finding allows for circumventing some experimental difficulty for direct determination of some thermodynamic properties of confined fluids. A challenge in perspective is to see if the scaling relation also holds for the fluid adsorption in flexible porous materials, for example, metal−organic frameworks, or to find the modifications needed if necessary.

■ APPENDIX

In this appendix, we provide the technique details about the models considered in this work and simulation method as well as calculation conditions.

5. Models

5.1. HS Fluid Confined in Various Porous Environments.

In the present work, we consider only a one-component fluid (denoted as species 1). The fluid−fluid interaction between HS particles of radius, R_1, is given by

$$u_{11}(|\mathbf{r}_i - \mathbf{r}_j|) = \begin{cases} \infty & |\mathbf{r}_i - \mathbf{r}_j| < 2R_1 \\ 0 & |\mathbf{r}_i - \mathbf{r}_j| \geq 2R_1 \end{cases} \tag{16}$$

where $\mathbf{r}_i$ and $\mathbf{r}_j$ are the position vectors of the ith and jth fluid particles, respectively. Various confining environments are considered. For the Madden−Glandt model of random porous matrices (denoted as species 0),[37] the following fluid−matrix interaction is considered:

$$u_{10}(|\mathbf{r} - \mathbf{q}_j|) = \begin{cases} \infty & |\mathbf{r} - \mathbf{q}_j| < R_0 + R_1 \\ \varepsilon_0 & R_0 + R_1 \leq |\mathbf{r} - \mathbf{q}_j| < R_0 + R_1 + d \\ 0 & |\mathbf{r} - \mathbf{q}_j| \geq R_0 + R_1 + d \end{cases} \tag{17}$$

where R_0 is the matrix particle radius, $\mathbf{q}_j$ the position vector of the jth matrix particle, and ε_0 and d are the potential well depth and width, respectively. In the case of $\varepsilon_0 = 0$ and $d = 0$, we have a HS matrix. The configurations of a HS matrix are generated from an equilibrium system with the following interaction:

$$u_{00}(|\mathbf{q}_i - \mathbf{q}_j|) = \begin{cases} \infty & |\mathbf{q}_i - \mathbf{q}_j| < 2R_0 \\ 0 & |\mathbf{q}_i - \mathbf{q}_j| \geq 2R_0 \end{cases} \tag{18}$$

For an OHS matrix, the matrix particles are placed totally randomly, that is, $u_{00}(|\mathbf{q}_i - \mathbf{q}_j|) = 0$. We also considered a slit pore with the width of L and the interaction between fluid and the pore wall is given by

$$w(z_i) = \begin{cases} \infty & |z_i| \geq (L - \sigma_1)/2 \\ \varepsilon_{10} & (L - \sigma_1)/2 - d \leq |z_i| < (L - \sigma_1)/2 \\ 0 & |z_i| < (L - \sigma_1)/2 - d \end{cases} \tag{19}$$

where $\sigma_1 = 2R_1$ and z_i is the coordinate along the coordinate axis perpendicular to the slit walls (note that the origin of the coordinate system is placed at the middle of the slit pore). In the case of $\varepsilon_{10} = 0$ and $d = 0$, we have the simple case of a slit pore with two hard walls. For slit pores, we calculate the fluid density by using the physical volume, that is, $V = AL$ (A: surface area), but not the volume accessible to the centers of fluid particles $[A(L - \sigma_1)]$.

5.2. LJ Fluid Confined in Various Porous Environments.

To demonstrate the validity of the scaling relation when an attractive fluid−fluid interaction is also present, an LJ fluid with the following interaction is considered as well:

$$u_{11}(|\mathbf{r}_i - \mathbf{r}_j|) = \begin{cases} u_{\mathrm{LJ}}(|\mathbf{r}_i - \mathbf{r}_j|) - u_{\mathrm{LJ}}(r_{11}^{\mathrm{c}}) & |\mathbf{r}_i - \mathbf{r}_j| \leq r_{11}^{\mathrm{c}} \\ 0 & |\mathbf{r}_i - \mathbf{r}_j| > r_{11}^{\mathrm{c}} \end{cases} \tag{20}$$

$$u_{\mathrm{LJ}}(r) = 4\varepsilon_1[(\sigma_1/r)^{12} - (\sigma_1/r)^6] \tag{21}$$

where $r_{11}^{\mathrm{c}} = 10R_1$, $\sigma_1 = 2R_1$, and ε_1 is the potential well depth. When this LJ fluid is confined in an LJ matrix, the fluid−matrix and matrix−matrix interactions are given, respectively, by

$$u_{10}(|\mathbf{r}_i - \mathbf{q}_j|) = \begin{cases} u_{\mathrm{LJ}}(|\mathbf{r}_i - \mathbf{q}_j|) - u_{\mathrm{LJ}}(r_{10}^{\mathrm{c}}) & |\mathbf{r}_i - \mathbf{q}_j| \leq r_{10}^{\mathrm{c}} \\ 0 & |\mathbf{r}_i - \mathbf{q}_j| > r_{10}^{\mathrm{c}} \end{cases} \tag{22}$$

$$u_{\mathrm{LJ}}(r) = 4\varepsilon_{10}[(\sigma_{10}/r)^{12} - (\sigma_{10}/r)^6] \tag{23}$$

and

$$u_{00}(|\mathbf{q}_i - \mathbf{q}_j|) = \begin{cases} u_{\mathrm{LJ}}(|\mathbf{q}_i - \mathbf{q}_j|) - u_{\mathrm{LJ}}(r_{00}^{\mathrm{c}}) & |\mathbf{q}_i - \mathbf{q}_j| \leq r_{00}^{\mathrm{c}} \\ 0 & |\mathbf{q}_i - \mathbf{q}_j| > r_{00}^{\mathrm{c}} \end{cases} \tag{24}$$

$$u_{\mathrm{LJ}}(r) = 4\varepsilon_0[(\sigma_0/r)^{12} - (\sigma_0/r)^6] \tag{25}$$

where $r_{00}^{\mathrm{c}} = 10R_0$, $\sigma_0 = 2R_0$, $r_{10}^{\mathrm{c}} = 5(R_1 + R_0)$, and ε_0 is the potential well depth for the matrix−matrix interaction. We considered the cases that $\varepsilon_0/\varepsilon_1 = 0.70$, 1.00, 1.75, 3.50, 5.25, and 7.00. σ_{10} and ε_{10} are obtained from the Lorentz−Berthelot mixing rule

$$\varepsilon_{10} = \sqrt{\varepsilon_0 \varepsilon_1} \tag{26}$$

$$\sigma_{10} = \frac{\sigma_1 + \sigma_0}{2} \tag{27}$$

Calculations have also been performed for an LJ fluid confined in a slit pore with hard walls. For an LJ matrix, we calculate the geometric porosity by $\phi_0 = 1 - \pi\rho_0\sigma_0^3/6$ ($\rho_0 = N_0/V$, N_0: number of matrix particles).

6. Method

Canonical ensemble Monte Carlo (CEMC) simulations are carried out for generating matrix configurations and those of a fluid confined in a particular matrix configuration. A cubic simulation box of volume V is used with a periodic boundary condition in three space directions when a fluid confined in a matrix is considered. For slit pores, the simulation box is made with two square walls separated by a distance equal to L and the periodic boundary condition is applied only in the two space directions parallel to the walls. For each simulation, about 2×10^5 to 1×10^6 trial moves for each fluid particle are performed. As finite size matrices are used, any observable quantity fluctuates with matrix realizations and an average made typically with about 10 matrix realizations leads to converged results. The excess chemical potential of the fluid, μ_1^{ex}, is calculated for different densities, ρ_1 ($\rho_1 = N_1/V$, N_1: number of fluid particles), by using Widom's test particle method.[73] Then, Helmholtz free energy is determined by a thermodynamic integration, that is,

$$\frac{\beta F}{N_1} = \ln(\rho_1 \Lambda_1^3) - 1 + \frac{1}{\rho_1}\int_0^{\rho_1} \beta\mu^{\mathrm{ex}}(\rho)\, \mathrm{d}\rho \tag{28}$$

where Λ_1 is the thermal wavelength of fluid particles and in this work, we set $\Lambda_1 = \sigma_1$. Finally, we obtain readily the compressibility factor from the following thermodynamic relation:

$$\frac{\beta\Omega}{N_1} = -\beta\mu + \frac{\beta F}{N_1} \tag{29}$$

7. Conditions of Considered Systems

The computational conditions of all the considered systems are summarized in Table 1. The confining environments considered in this work can be classified into two big categories: (i) porous matrices and (ii) slit pores. According to their different morphologies of pore space, we can divide porous matrices into four different types. Disordered porous matrices are generated by quenching an equilibrium system according to the procedure proposed by Madden and Glandt[37] and denoted, in Table 1, as HSM_d if the matrix−matrix interaction is HS one or LJM_d when the matrix−matrix interaction is LJ one. In contrast, ordered porous matrices can be generated by arranging a matrix particle into an ordered structure. In this work, we only studied the case that matrix particles are placed on a simple cubic lattice and the acronyms used for such matrices are HSM_o (HS for fluid−matrix interaction) and LJM_o (LJ for fluid−matrix interaction). The third type of matrices we considered is a templated matrix. According to the procedure proposed by Van Tassel and Zhang,[38,39] a templated matrix is obtained by quenching an equilibrium binary system and removing one of its components after quenching. We considered only a templated HS matrix, denoted by THSM in Table 1, with the same number of templates and matrix particles, and moreover, they have the same size. The fourth type of matrices is the hard sponge one,[41,49] denoted as HSG in Table 1.

Table 1. Computation Parameters for Canonical Ensemble or Grand Canonical Ensemble Monte-Carlo Simulations

Pore	f-s	f-f	τ	T^*	Symbol
Slit (width: 5)	HW	HS	-	-	●
Slit (width: 5)	SW(1,-1)	HS	-	1	●
Slit (width: 5)	SW(1,1)	HS	-	1	●
Slit (width: 3.5)	HW	HS	-	-	●
Slit (width: 7)	HW	HS	-	-	●
HSM_d (ρ_0^*=0.2)	HS	HS	0.5	-	●
HSM_d (ρ_0^*=0.55)	HS	HS	0.2	-	●
HSM_d (ρ_0^*=0.25)	SW(1,-1)	HS	0.2	1	●
HSM_d (ρ_0^*=0.25)	SW(1,1)	HS	0.2	1	●
HSM_d (ρ_0^*=0.5)	SW(1,-1)	HS	0.1	1	●
HSM_d (ρ_0^*=0.5)	SW(1,1)	HS	0.1	1	●
HSM_o (ρ_0^*=0.578)	SW(1,-2)	HS	0.1	1	●
HSM_o (ρ_0^*=0.578)	SW(1,2)	HS	0.1	1	●
HSM_o (ρ_0^*=0.125)	HS	HS	0.2	-	●
HSM_o (ρ_0^*=0.75)	HS	HS	0.1		●
THSM (ρ_0^*=0.2)	HS	HS	0.5	-	●
THSM (ρ_0^*=0.15)	HS	HS	0.2	-	●
THSM (ρ_0^*=0.5)	HS	HS	0.1	-	●
HSG (ρ_0^*=1.172)	HSG	HS	0.1	-	●
Slit (width: 5)	HW	LJ (1)	-	3.5	●
LJM_d (ρ_0^*=0.25)	LJ (1)	LJ (1)	0.2	3.5	●
LJM_d (ρ_0^*=0.5)	LJ (1)	LJ (1)	0.1	3.5	●
LJM_o (ρ_0^*=0.5)	LJ (1)	LJ (1)	0.2	3.5	●
LJM_d (ρ_0^*=0.5)	LJ ($\sqrt{1.75}$)	LJ (1)	0.2	3.5	●
LJM_d (ρ_0^*=0.5)	LJ ($\sqrt{0.7}$)	LJ (1)	0.2	3.5	●
LJM_d (ρ_0^*=0.5)	LJ ($\sqrt{3.5}$)	LJ (1)	0.2	3.5	●
LJM_d (ρ_0^*=0.5)	LJ ($\sqrt{7}$)	LJ (1)	0.2	3.5	●
LJM_d (ρ_0^*=0.5)	LJ ($\sqrt{5.25}$)	LJ (1)	0.2	3.5	●

The meaning of the title labels in Table 1 is the following:

f−s: fluid−solid interaction (here, the word "solid" is used to denote either a hard wall or matrix particles);

f−f: fluid−fluid interaction;

τ: fluid matrix particle size ratio, σ_1/σ_0;

T^*: temperature, $T^* = k_BT/\varepsilon_{\text{ref}}$ (ε_{ref}: reference energy unit, all the well depth parameters for square well or LJ potentials, for example, ε_0, ε_1, are defined with respect to this reference unit);

Symbol: symbols used for curves plotted in different figures of the paper.

The definitions of all the other reduced parameters given in Table 1 are given below as well.

Slit width: $L^* = L/\sigma_1$;

SW(d^*,ε_{10}^*): square well potential with width, $d^* = d/\sigma_1$, and depth, $\varepsilon_{10}^* = \varepsilon_{10}/\varepsilon_{\text{ref}}$;

LJ(ε^*): LJ potential with depth, $\varepsilon^* = \varepsilon_1/\varepsilon_{\text{ref}}$ (for fluid−fluid interaction) or $\varepsilon^* = \varepsilon_{10}/\varepsilon_{\text{ref}}$ (for fluid−matrix interaction);

ρ_0^*: matrix density, $\rho_0^* = \rho_0\sigma_0^3$ ($\rho_0 = N_0/V$, N_0: number of matrix particles).

■ AUTHOR INFORMATION

Corresponding Authors

*E-mail: szhao@ecust.edu.cn (S.L.Z.).
*E-mail: wei.dong@ens-lyon.fr (W.D.).

ORCID

S. L. Zhao: 0000-0002-9547-4860
H. L. Liu: 0000-0002-5682-2295
W. Dong: 0000-0003-3773-1029

Notes

The authors declare no competing financial interest.

■ ACKNOWLEDGMENTS

This research is supported partially by the National Science Foundation of China (nos. 21878078 and U1707602) and by the 111 Project of China (grant no. B08021). S.L.Z. acknowledges the support from the Fok Ying Tong Education Foundation (151069). C.Z.Q. is grateful to Campus France for an Eiffel scholarship, to la Région Rhône-Alpes (France) for a CMIRA scholarship, and to the Chinese Scholarship Council for the visiting fellowship.

■ REFERENCES

(1) Davis, M. E. Ordered porous materials for emerging applications. *Nature* **2002**, *417*, 813−821.

(2) Férey, G. Hybrid porous solids: past, present, future. *Chem. Soc. Rev.* **2008**, *37*, 191−214.

(3) Schlapbach, L.; Züttel, A. Hydrogen-storage materials for mobile applications. *Nature* **2001**, *414*, 353−358.

(4) Corma, A. From microporous to mesoporous molecular sieve materials and their use in catalysis. *Chem. Rev.* **1997**, *97*, 2373−2420.

(5) Brennan, J. K.; Thomson, K. T.; Gubbins, K. E. Adsorption of water in activated carbons: Effects of pore blocking and connectivity. *Langmuir* **2002**, *18*, 5438−5447.

(6) Palmer, J. C.; Moore, J. D.; Brennan, J. K.; Gubbins, K. E. Simulating local adsorption isotherms in structurally complex porous materials: A direct assessment of the slit pore model. *J. Phys. Chem. Lett.* **2011**, *2*, 165−169.

(7) Gubbins, K. E.; Liu, Y.-C.; Moore, J. D.; Palmer, J. C. The role of molecular modeling in confined systems: impact and prospects. *Phys. Chem. Chem. Phys.* **2011**, *13*, 58−85.

(8) Fernaud, M. J.; Lomba, E.; Martín, C.; Levesque, D.; Weis, J.-J. Study of dipolar fluid inclusions in charged random matrices. *J. Chem. Phys.* **2003**, *119*, 364.

(9) Almarza, N. G.; Gallardo, A.; Martín, C.; Guil, J. M.; Lomba, E. Topological considerations on microporous adsorption processes in simple models for pillared interlayered clays. *J. Chem. Phys.* **2009**, *131*, 244701.

(10) Lomba, E.; Weis, J.-J. A computational study of electrolyte adsorption in a simple model for intercalated clays. *J. Chem. Phys.* **2010**, *132*, 104705.

(11) Lomba, E.; Bores, C.; Kahl, G. Explicit spatial description of fluid inclusions in porous matrices in terms of an inhomogeneous integral equation. *J. Chem. Phys.* **2014**, *141*, 164704.

(12) Lomba, E.; Bores, C.; Sánchez-Gil, V.; Noya, E. G. A three dimensional integral equation approach for fluids under confinement: Argon in zeolites. *J. Chem. Phys.* **2015**, *143*, 164703.

(13) Paschinger, E.; Kahl, G. Structure and thermodynamic properties of a binary liquid in a porous matrix: The formalism. *Phys. Rev. E: Stat. Phys., Plasmas, Fluids, Relat. Interdiscip. Top.* **2000**, *61*, 5330−5338.

(14) Schöll-Paschinger, E.; Levesque, D.; Weis, J.-J.; Kahl, G. Phase diagram of a symmetric binary fluid in a porous matrix. *Phys. Rev. E: Stat., Nonlinear, Soft Matter Phys.* **2001**, *64*, 011502.

(15) Schmidt, M.; Schöll-Paschinger, E.; Köfinger, J. r.; Kahl, G. Model colloid polymer mixtures in porous matrices: density functional versus integral equations. *J. Phys.: Condens. Matter* **2002**, *14*, 12099−12117.

(16) Bores, C.; Almarza, N. G.; Lomba, E.; Kahl, G. Inclusions of a two dimensional fluid with competing interactions in a disordered, porous matrix. *J. Phys.: Condens. Matter* **2015**, *27*, 194127.

(17) Schwanzer, D. F.; Coslovich, D.; Kurzidim, J.; Kahl, G. Effects of porous confinement on the structural properties of the Gaussian core model. *Mol. Phys.* **2009**, *107*, 433.

(18) Kurzidim, J.; Coslovich, D.; Kahl, G. Impact of random obstacles on the dynamics of a dense colloidal fluid. *Phys. Rev. E: Stat., Nonlinear, Soft Matter Phys.* **2010**, *82*, 041505.

(19) Kurzidim, J.; Kahl, G. Accessible volume in quenched-annealed mixtures of hard spheres: a geometric decomposition. *Mol. Phys.* **2011**, *109*, 1331−1342.

(20) Vega, C.; Kaminsky, R. D.; Monson, P. A. Adsorption of fluids in disordered porous media from integral equation theory. *J. Chem. Phys.* **1993**, *99*, 3003.

(21) Padilla, P.; Vega, C. Adsorption isotherm for flexible molecules in random porous media. Can we regard the system as a binary mixture? *J. Chem. Phys.* **1997**, *106*, 1997−2011.

(22) Padilla, P.; Pizio, O.; Trokhymchuk, A.; Vega, C. Adsorption of dimerizing and dimer fluids in disordered porous media. *J. Phys. Chem. B* **1998**, *102*, 3012.

(23) Padilla, P.; Vega, C.; Pizio, O.; Trokhymchuk, A. The structure and adsorption of diatomic fluids in disordered porous media. A Monte Carlo simulation study. *Mol. Phys.* **1998**, *95*, 701.

(24) Brennan, J. K.; Dong, W. Phase transitions of one-component fluids adsorbed in random porous media: Monte Carlo simulations. *J. Chem. Phys.* **2002**, *116*, 8948−8958.

(25) Brennan, J. K.; Dong, W. Molecular simulation of the vapor-liquid phase behavior of Lennard-Jones mixtures in porous solids. *Phys. Rev. E: Stat., Nonlinear, Soft Matter Phys.* **2003**, *67*, 031503.

(26) Vakarin, E. V.; Dong, W.; Badiali, J. P. On the double phase-transition of fluids adsorbed in disordered porous media. *Phys. A* **2007**, *379*, 389.

(27) Tolman, R. C. The effect of droplet size on surface tension. *J. Chem. Phys.* **1949**, *17*, 333−337.

(28) Bryk, P.; Roth, R.; Mecke, K. R.; Dietrich, S. Hard-sphere fluids in contact with curved substrates. *Phys. Rev. E: Stat., Nonlinear, Soft Matter Phys.* **2003**, *68*, 031602.

(29) König, P.-M.; Roth, R.; Mecke, K. R. Morphological thermodynamics of fluids: shape dependence of free energies. *Phys. Rev. Lett.* **2004**, *93*, 160601.

(30) Mecke, K.; Rauscher, M. On thermal fluctuations in thin film flow. *J. Phys.: Condens. Matter* **2005**, *17*, S3515−S3522.

(31) Hansen-Goos, H.; Roth, R.; Mecke, K.; Dietrich, S. Solvation of proteins: linking thermodynamics to geometry. *Phys. Rev. Lett.* **2007**, *99*, 128101.

(32) Reindl, A.; Bier, M.; Dietrich, S. Implications of interface conventions for morphometric thermodynamics. *Phys. Rev. E: Stat., Nonlinear, Soft Matter Phys.* **2015**, *91*, 022406.

(33) Laird, B. B.; Hunter, A.; Davidchack, R. L. Interfacial free energy of a hard-sphere fluid in contact with curved hard surfaces. *Phys. Rev. E: Stat., Nonlinear, Soft Matter Phys.* **2012**, *86*, No. 060602(R).

(34) Blokhuis, E. M. Existence of a bending rigidity for a hard-sphere liquid near a curved hard wall: Validity of the Hadwiger theorem. *Phys. Rev. E: Stat., Nonlinear, Soft Matter Phys.* **2013**, *87*, 022401.

(35) Urrutia, I. Bending rigidity and higher-order curvature terms for the hard-sphere fluid near a curved wall. *Phys. Rev. E: Stat., Nonlinear, Soft Matter Phys.* **2014**, *89*, 032122.

(36) Hansen-Goos, H. Communication: Non-Hadwiger terms in morphological thermodynamics of fluids. *J. Chem. Phys.* **2014**, *141*, 171101.

(37) Madden, W. G.; Glandt, E. D. Distribution functions for fluids in random media. *J. Stat. Phys.* **1988**, *51*, 537−558.

(38) Van Tassel, P. R. Theoretical studies of the available volume for adsorption in a random quenched and depleted disordered medium. *J. Chem. Phys.* **1997**, *107*, 9530−9534.

(39) Zhang, L.; Van Tassel, P. R. Theory and simulation of adsorption in a templated porous material: Hard sphere systems. *J. Chem. Phys.* **2000**, *112*, 3006.

(40) Dong, W.; Kierlik, E.; Rosinberg, M. L. Integral equations for a fluid near a random substrate. *Phys. Rev. E: Stat. Phys., Plasmas, Fluids, Relat. Interdiscip. Top.* **1994**, *50*, 4750−4753.

(41) Zhao, S. L.; Dong, W.; Liu, Q. H. Fluids in porous media. I. A hard sponge model. *J. Chem. Phys.* **2006**, *125*, 244703.

(42) Dong, W.; Krakoviack, V.; Zhao, S. L. Fluids Confined in Porous Media: A Soft-Sponge Model†. *J. Phys. Chem. C* **2007**, *111*, 15910−15923.

(43) Zhao, S. L.; Dong, W.; Liu, Q. H. A new model of templated porous materials. *J. Mol. Liq.* **2007**, *136*, 241−248.

(44) Dong, W. Mechanical route to the pressure of a fluid adsorbed in a random porous medium. *J. Chem. Phys.* **1995**, *102*, 6570−6573.

(45) Dong, W.; Chen, X. S.; Zheng, W. M. Thermodynamic pressure of a fluid confined in a random porous medium. *Phys. Rev. E: Stat., Nonlinear, Soft Matter Phys.* **2005**, *72*, 012201.

(46) Holovko, M.; Dong, W. A highly accurate and analytic equation of state for a hard sphere fluid in random porous media. *J. Phys. Chem. B* **2009**, *113*, 6360−6365.

(47) Chen, W.; Dong, W.; Holovko, M.; Chen, X. S. Comment on "A Highly Accurate and Analytic Equation of State for a Hard Sphere Fluid in Random Porous Media". *J. Phys. Chem. B* **2010**, *114*, 1225.

(48) Patsahan, T.; Holovko, M.; Dong, W. Fluids in porous media. III. Scaled particle theory. *J. Chem. Phys.* **2011**, *134*, 074503.

(49) Holovko, M.; Patsahan, T.; Dong, W. Fluids in random porous media: Scaled particle theory. *Pure Appl. Chem.* **2013**, *85*, 115−133.

(50) Chen, W.; Zhao, S. L.; Holovko, M.; Chen, X. S.; Dong, W. Scaled particle theory for multicomponent hard sphere fluids confined in random porous media. *J. Phys. Chem. B* **2016**, *120*, 5491−5504.

DOI: 10.1021/acs.langmuir.8b03126
Langmuir 2019, 35, 3840−3847

(51) Dong, W.; Chen, X. Scaled particle theory for bulk and confined fluids: A review. *Sci. China: Phys., Mech. Astron.* **2018**, *61*, 070501.
(52) Lomba, E.; Given, J. A.; Stell, G.; Weis, J. J.; Levesque, D. Ornstein-Zernike equations and simulation results for hard-sphere fluids adsorbed in porous media. *Phys. Rev. E: Stat. Phys., Plasmas, Fluids, Relat. Interdiscip. Top.* **1993**, *48*, 233.
(53) Fernaud, M.-J.; Lomba, E.; Lee, L. L. Chemical potentials and potential distributions of inclusion gas in quenched-annealed random porous media. *J. Chem. Phys.* **1999**, *111*, 10275−10286.
(54) Fernaud, M. J.; Lomba, E.; Weis, J. J. Adsorption of a diatomic molecular fluid into random porous media. *Phys. Rev. E: Stat., Nonlinear, Soft Matter Phys.* **2001**, *64*, 051501.
(55) Rosinberg, M. L.; Tarjus, G.; Stell, G. Thermodynamics of fluids in quenched disordered matrices. *J. Chem. Phys.* **1994**, *100*, 5172−5177.
(56) Kierlik, E.; Rosinberg, M. L.; Tarjus, G.; Monson, P. The pressure of a fluid confined in a disordered porous material. *J. Chem. Phys.* **1995**, *103*, 4256−4260.
(57) Kierlik, E.; Rosinberg, M. L.; Tarjus, G.; Monson, P. A. Phase diagrams of single-component fluids in disordered porous materials: Predictions from integral-equation theory. *J. Chem. Phys.* **1997**, *106*, 264.
(58) Kierlik, E.; Rosinberg, M. L.; Tarjus, G.; Pitard, E. Mean-spherical approximation for a lattice model of a fluid in a disordered matrix. *Mol. Phys.* **1998**, *95*, 341.
(59) Krakoviack, V.; Kierlik, E.; Rosinberg, M.-L.; Tarjus, G. Adsorption of a fluid in an aerogel: Integral equation approach. *J. Chem. Phys.* **2001**, *115*, 11289−11298.
(60) Krakoviack, V. Liquid-glass transition of a fluid confined in a disordered porous matrix: A mode-coupling theory. *Phys. Rev. Lett.* **2005**, *94*, 065703.
(61) Krakoviack, V. Mode-coupling theory for the slow collective dynamics of fluids adsorbed in disordered porous media. *Phys. Rev. E: Stat., Nonlinear, Soft Matter Phys.* **2007**, *75*, 031503.
(62) Krakoviack, V. Tagged-particle dynamics in a fluid adsorbed in a disordered porous solid: Interplay between the diffusion-localization and liquid-glass transitions. *Phys. Rev. E: Stat., Nonlinear, Soft Matter Phys.* **2009**, *79*, 061501.
(63) Yethiraj, A. Integral equations for polymers in quenched random media. *J. Chem. Phys.* **2002**, *116*, 5910−5911.
(64) Sung, B. J.; Yethiraj, A. Monte Carlo simulation and self-consistent integral equation theory for polymers in quenched random media. *J. Chem. Phys.* **2005**, *123*, 074909.
(65) Johnson, J. K.; Zollweg, J. A.; Gubbins, K. E. The Lennard-Jones equation of state revisited. *Mol. Phys.* **1993**, *78*, 591−618.
(66) Gibbs, J. W. *Collected Works*; Longmans Green and Company: New York, 1928; Vol. *1*.
(67) Rowlinson, J. S.; Widom, B. *Molecular Theory of Capillarity*; Oxford University Press: New York, 1982.
(68) Mittal, J.; Errington, J. R.; Truskett, T. M. Thermodynamics predicts how confinement modifies the dynamics of the equilibrium hard-sphere fluid. *Phys. Rev. Lett.* **2006**, *96*, 177804.
(69) Mittal, J.; Errington, J. R.; Truskett, T. M. Does confining the hard-sphere fluid between hard walls change its average properties? *J. Chem. Phys.* **2007**, *126*, 244708.
(70) Mittal, J. Using Compressibility Factor as a Predictor of Confined Hard-Sphere Fluid Dynamics†. *J. Phys. Chem. B* **2009**, *113*, 13800−13804.
(71) Borah, B. J.; Maiti, P. K.; Chakravarty, C.; Yashonath, S. Transport in nanoporous zeolites: Relationships between sorbate size, entropy, and diffusivity. *J. Chem. Phys.* **2012**, *136*, 174510.
(72) Ingebrigtsen, T. S.; Errington, J. R.; Truskett, T. M.; Dyre, J. C. Predicting how nanoconfinement changes the relaxation time of a supercooled liquid. *Phys. Rev. Lett.* **2013**, *111*, 235901.
(73) Allen, M. P.; Tildesley, D. J. *Computer Simulation of Liquids*; Oxford University Press: New York, 1987.